

Improved *in situ* isotope analysis of low-Pb materials using LA-MC-ICP-MS with parallel ion counter and Faraday detection

Bence Paul,* Jon D. Woodhead and Janet Hergt

School of Earth Sciences, The University of Melbourne, Melbourne, VIC 3010, Australia.

E-mail: b.paul@pgrad.unimelb.edu.au; Fax: +61 3 8344 7761; Tel: +61 3 8344 6911

Received 31st May 2005, Accepted 6th September 2005

First published as an Advance Article on the web 26th September 2005

A new analytical protocol is described allowing the measurement of Pb-isotope ratios, including the low abundance isotope ^{204}Pb , in relatively small targets (~ 100 micron) of low Pb content (1–10 ppm), such as might be encountered in the analysis of magmatic melt inclusions, for example. The analysis routine employed utilises multiple Faraday cups and two ion counters operated in static multi-collection mode. Concurrent analysis of the NIST 612 glass standard allows an external correction for mass bias, and simultaneous determination of ion counter gain, while Hg interference on ^{204}Pb is corrected in real time by simultaneous acquisition of ^{200}Hg in a second ion counter. Analytical precision approximates theoretical limits and it can be shown that analytical accuracy is limited primarily by ion counter gain for ratios involving ^{204}Pb and the mass bias correction for all other ratios. We typically obtain precisions of $<0.4\%$ RSD (2 sigma) and accuracy of $\leq 0.2\%$ on BCR2-g for ratios involving ^{204}Pb . Two other glass reference materials (MPI-DING ATHO-G and KL2-G) were also analysed, and precision of $\leq 1.8\%$ RSD (2 sigma) and accuracy of $\leq 0.9\%$ were obtained for the glass with the lowest Pb abundance of approximately $2 \mu\text{g g}^{-1}$. These results provide an improvement on the accuracy and precision of laser ablation ratio determinations, attributable to stable instrument conditions and high sensitivity.

Introduction

Laser ablation inductively coupled plasma mass spectrometry (LA-ICP-MS) has been demonstrated as a powerful tool for documenting elemental and isotopic variation at scales down to $\sim 10 \mu\text{m}$. The technology was quickly adopted for *in situ* Pb-isotope analysis,^{1,2} and has been applied to a variety of problems, ranging from archaeological investigations of Roman coins³ to documenting Pb isotopic disequilibrium in igneous systems (e.g. Mathez and Waight⁴) and U–Pb geochronology (e.g. Horn *et al.*⁵). Despite these advances, the measurement of Pb-isotope ratios by LA-ICP-MS, is not without difficulties. Whereas many isotope systems have an invariant isotope pair with which to correct for instrumental mass bias effects, the Pb system does not, a limitation quickly recognised by early investigators.¹ In addition, measurement of the stable isotope ^{204}Pb , is compromised not only by its relatively low abundance ($\sim 1.4\%$ of total Pb in most samples but often far less in radiogenic materials), but also by a potentially severe isobaric interference from ^{204}Hg . While for the purpose of U–Pb geochronology alternative solutions have been explored which do not require the measurement of ^{204}Pb (e.g. Andersen,⁶ Jackson *et al.*⁷), the difficulty in measuring ratios involving ^{204}Pb is a particularly significant impediment for the use of Pb-isotopes in tracer studies and Pb–Pb geochronology where the radiogenic isotopes ^{206}Pb , ^{207}Pb , and ^{208}Pb are usually reported relative to this isotope.

Recently Horstwood *et al.*⁸ described an analytical protocol for U–Pb geochronology of accessory phases in which they monitored ^{204}Pb in order to correct for any common Pb contribution. In their study, however, extremely high precision measurements of the $^{206}\text{Pb}/^{204}\text{Pb}$ ratios were not required (such high precision data are unnecessary for the bulk of geochronological applications). In our laboratory we typically use Pb-isotope analysis for petrogenetic studies where high-precision analysis is often a necessity and, most recently, have

attempted to apply this approach *in situ* to extremely small samples such as magmatic melt inclusions trapped in olivines (which are typically tens to hundreds of microns in size). Any attempt to analyse these materials using laser ablation requires very rapid analysis times and led us to develop a new methodology allowing the simultaneous (static) measurement of all Pb isotopes including ^{204}Pb . A 193 nm excimer laser and He ablation environment has been utilised to provide high sensitivity (e.g. Eggins *et al.*⁹), while both measurement of ^{204}Pb and an on-line correction for Hg-interference is accomplished by the use of parallel ion counters used in tandem with measurement of the more abundant isotopes in Faraday cups. The utility of this technique and the levels of analytical precision/accuracy obtained are demonstrated by the analysis of a variety of glass standards of variable Pb concentration ranging from 2 to 10 ppm, with spot sizes, ablation rates, and analysis times chosen to simulate the analysis of glassy melt inclusions. These glass reference materials were first characterised using conventional solution mode methods to allow comparison with the *in situ* results.

Experimental

Sample preparation and instrumentation

Samples measured in solution mode were prepared and analysed according to the procedures documented by Woodhead,¹⁰ employing anion exchange chemistry and internal Tl mass bias correction. For *in situ* analyses, glass chips were mounted in epoxy resin blocks, and polished to a flat surface. Each mount was carefully cleaned with methanol to reduce surficial contamination before being placed in the ablation cell.

All analyses, in both solution and laser sampling modes, were conducted on a “Nu Plasma” MC-ICP-MS (Nu Instruments, Wrexham, UK). This instrument has a detection system incorporating twelve Faraday cups and three ETP electron

Table 1 Typical operating conditions for the Nu Plasma instrument (a), and collector assignments for *in situ* and solution Pb analyses (b)

(a) Typical instrument operating conditions															
Nu Plasma MC-ICP-MS															
Forward power	1350 W														
Reflected power	<2 W														
Accelerating voltage	4000 V														
Analyser pressure	4×10^{-9} mbar														
Cones	Ni														
Plasma gas	13 l min ⁻¹														
Auxiliary gas	0.90 l min ⁻¹														
Nebuliser gas	0.85 l min ⁻¹														
HelEx laser ablation system															
Lambda Physik Compex 110 ArF excimer	193 nm														
Laser fluence	~ 5 J cm ⁻²														
Spot size	93 μm														
Repetition rate	6 Hz														
He gas to cell	200 ml min ⁻¹														
(b) Nu Plasma collector assignments for Pb-isotope analyses															
Collector ^a	H6	H5	H4	H3	H2	H1	Ax	L1	L2	IC0	L3	IC1	L4	IC2	L5
Laser ablation															
Analyte isotopes						²⁰⁸ Pb	²⁰⁷ Pb	²⁰⁶ Pb	²⁰⁵ Tl ^b	²⁰⁴ Pb	²⁰³ Tl				
Gas-related interferences										²⁰⁴ Hg				²⁰⁰ Hg	
Solution															
Analyte isotopes			²⁰⁸ Pb	²⁰⁷ Pb	²⁰⁶ Pb	²⁰⁵ Tl	²⁰⁴ Pb	²⁰³ Tl							
Gas-related interferences							²⁰⁴ Hg		²⁰² Hg						
^a Collectors H6 to H1, Ax, and L1 to L5 are Faraday cups, IC0 to IC2 are ion counters. ^b Although Tl is measured, its concentration in samples is too low to be utilised in mass fractionation calculations.															

^a Collectors H6 to H1, Ax, and L1 to L5 are Faraday cups, IC0 to IC2 are ion counters. ^b Although Tl is measured, its concentration in samples is too low to be utilised in mass fractionation calculations.

multiplier ion counters. In addition, an Edwards E2M80 rotary vacuum pump has replaced the original Edwards E2M28 pump to the sampler/skimmer interface to provide increased sensitivity. Typical analytical conditions for both solution and laser analyses are documented in Table 1. Faraday collectors are used to measure the ²⁰⁸Pb, ²⁰⁷Pb and ²⁰⁶Pb beams, and ²⁰⁵Tl and ²⁰³Tl. For solution analyses, where Hg interferences at $m/z = 204$ are negligible (typical ²⁰⁰Hg intensity for solutions is only ~ 800 cps), and samples are generally large, ²⁰⁴Pb is also measured in a Faraday cup. For laser sampling, however, when ²⁰⁴Pb is far smaller and significantly affected by Hg interference, ²⁰⁴X (where X is a combination of Pb and Hg), and ²⁰⁰Hg are both measured using ion counters. After an instrument warm-up period of around 30 minutes, gas flows, torch position, and focussing potentials are all optimised to provide the greatest sensitivity.

For *in situ* analyses, the MC-ICP-MS is coupled to a HelEx (Laurin Technic, Canberra, Australia, and the Australian National University) laser ablation system, incorporating a Compex 110 (Lambda Physik, Gottingen, Germany) excimer laser operating at 193 nm (see Table 1). A detailed description of the HelEx system is the subject of a separate publication by the Australian National University group, but discussion of its general characteristics and applications can be found in Eggins *et al.*⁹ and Woodhead *et al.*^{11,12} A spot size of 93 μm has been used for all samples and standards in this study, with a constant repetition rate of 6 Hz and laser fluence of approximately 5 J cm^{-2} . Backgrounds were measured 'on peak' for 60 s before each analysis with the carrier gas flowing but with the laser's shutter closed. All samples were measured with 60 s integration time, for a total of approximately 72 s total analysis time, allowing for 12 s wash-in (see Fig. 1). The integration time of 60 s was chosen as representative for analysis of very small samples of finite thickness *e.g.* melt inclusions, for which this project was initiated. Sensitivity, ablating a 93 μm spot, at a 6 Hz repetition rate, is approximately 60 mV ²⁰⁶Pb for NIST SRM 612 during the first 10 s of ablation. Blank levels for the

entire system are variable from day to day but are typically around 30–40 000 cps ²⁰⁰Hg at the start of a session and gradually decrease during the day, unless further Hg is contributed from ablation of samples. Such levels are rather high in comparison to many laboratories and have proved difficult to eliminate (a problem still under investigation). However, as will be demonstrated, they pose no serious impediment to the accurate and precise determination of Pb-isotope ratios. In the HelEx system the sample is ablated in an ultra-pure He environment and then rapidly entrained into the carrier Ar flow for transit to the ICP torch. Helium ablation reduces sample re-deposition and elemental fractionation¹³ and thus results in greater sensitivity.⁹ Several samples can be placed in the sample cell simultaneously, yet the volume of gas that the ablated material is exposed to is very small (~ 2 ml). This is significant since we have found that after changing samples, and evacuating the cell, it can take tens of minutes for Hg levels to stabilise, and thus this operation is best limited during any particular analytical session. A signal smoothing device, consisting of a number of bifurcating tubes of different path-length which are subsequently recombined (the 'squid') is incorporated between the cell and the torch, and although this adds a small contribution to the Hg background and increases the cell response time from <2 s to ~ 12 s, the resultant signal smoothing has been found to improve the overall reproducibility of results (see Fig. 1). Gold traps are placed before the cell on the argon and helium gas lines and help to reduce the Hg blank by around 50%. In addition, all gas and sample tubing (nylon) is periodically washed in a Citranox solution to remove contaminants that may build up after long periods of ablation experiments.

Analytical protocol and data reduction

In addition to peak-stripping of the Hg interference on ²⁰⁴Pb, two significant corrections must be applied to the measured

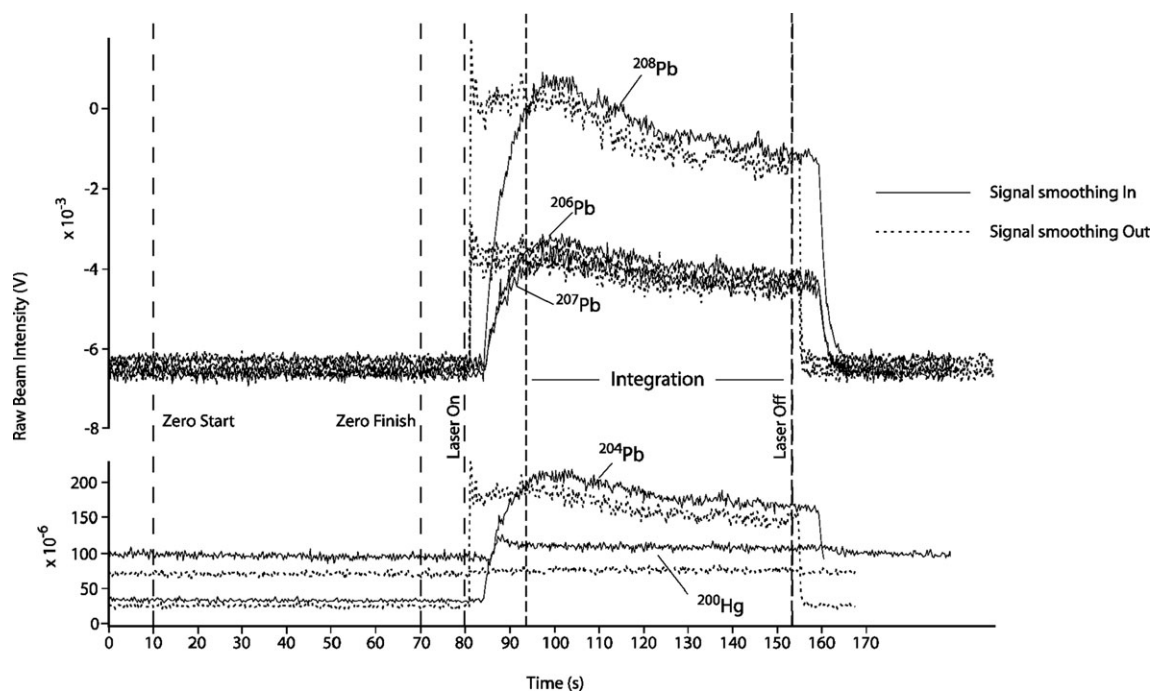


Fig. 1 Ion beam intensities *versus* time during a typical laser ablation run of an extremely low Pb sample. The laser shutter is opened at $t = 80$ s. The signal smoothing device contributes to the analytical blank, although it clearly provides significant improvement in signal stability. Total analysis time is less than three minutes per sample.

data to compensate for instrumental mass bias and ion counter gain, respectively; we discuss each in turn below.

Over the past few decades at least three different methods have been proposed to correct for instrumental mass bias effects encountered during Pb-isotope analysis. Arguably the most precise data are obtained by double- or triple-spike techniques which have been used for a number of years in TIMS analysis^{14,15} and also recently adapted for MC-ICP-MS solution work.¹⁶ Alternatively, it has become commonplace in solution MC-ICP-MS studies to add a Tl internal standard to monitor and ultimately correct for any mass bias effects.^{10,17,18} Some authors, in particular those attempting U–Pb geochronology on quadrupole ICP-MS instruments (*e.g.* Horn *et al.*⁵) have adopted a similar strategy by simultaneously aspirating a Tl-solution which is subsequently fed into the carrier gas flow from the ablation cell. The assumption is that all bias effects are a result of instrumental influences and, as a consequence, any changes observed in the Tl solution will be a reflection of those experienced by the Pb stream from the ablation cell. Philosophically this is certainly an attractive solution to the problem. However we have observed that neither our Aridus desolvation system nor laser cell can be operated with optimum gas flows when connected together in this way (Horn *et al.*⁵ came to a similar conclusion with the Meinhard nebuliser system). Perhaps as a result of this we see no evidence that Pb bias is related in any simple way to Tl bias for materials analysed using this approach, and, in addition, the combined gas flows can result in unstable Hg backgrounds which are highly undesirable for our method using ‘on peak zeros’. As a result we have resorted to a simple external normalisation protocol as originally used in TIMS Pb-isotope analysis and in some recent laser studies (*e.g.* Tiepolo;¹⁸ Willigers *et al.*¹⁹). Although largely unsuitable for ultra-high precision solution analyses such a method does provide a correction which is sufficiently accurate for laser ablation analyses, where other sources of error may dominate the total analytical uncertainty.

Since this work was ultimately developed for the analysis of very small glass inclusions, we use the NIST SRM 612 glass as an external standard, measured five times at the beginning of every analytical session, and three times between every five

‘unknowns’ thereafter. NIST SRM 612 was chosen for its relatively low Pb concentration²⁰ of $38.6 \mu\text{g g}^{-1}$ to more closely match the Pb concentrations of samples under study, while still providing adequate signal strength. From these analyses, mass bias is estimated simply by comparison of the ratio of two isotopes both measured in Faraday cups (typically $^{208}\text{Pb}/^{206}\text{Pb}$) with the ‘true’ ratio²¹ and using an exponential mass bias law. The relative gains of the Faraday cup amplifiers are determined each session using the instrument’s standard calibration routine; cup efficiencies are assumed to be invariant and equal. Variation in mass bias during an analytical session is generally very small, typically amounting to 4% drift in the exponential bias factor, ‘ F ’ over a period of six hours, a characteristic feature of plasma source spectrometers. A simple linear fit through the bias values obtained for the session then provides a bias estimate to be applied to any unknowns run concurrently.

During measurement of Pb-isotope ratios involving the minor isotope ^{204}Pb , small-scale variations in ion counter gain (at the 0.1–0.5% level), occurring on a short time-scale (*i.e.* during a single analytical session) are highly significant and must be monitored. Estimation of the ion counter gain can, in theory, be accomplished in a number of ways. Typically this might involve two cycles in which a given isotope pair is measured first in a Faraday–Faraday configuration and then again in Faraday–ion counter mode. Alternatively a single isotope can be jumped sequentially through a Faraday cup and ion counters. However, on the Nu Plasma with its novel zoom lens system, such approaches require minor adjustments to steering potentials between jumps to maintain optimum peak shape/alignment, and we prefer to make the ion counter gain determination using conditions identical to those under which we run samples, since steering of the ion beams into the electron multipliers is unlikely to be 100% efficient. For this reason we have found it simpler to estimate the ion counter gain from static measurements of SRM 612 which has a known Pb-isotope composition.²¹ In practice only the gain for IC0 (which monitors mass 204) needs to be determined to a high degree of precision since IC2 is only used to monitor and ultimately strip an extremely small contribution of Hg from ^{204}Pb , residual after the on peak zero. Consequently in this

method we adopt an average value for the gain on IC2 determined once at the beginning of each analytical session using solution nebulisation. The Hg mass bias factor is then determined on the cell gas flow, without ablation, using only ^{202}Hg and ^{200}Hg steered into IC0 and IC2. These average values for IC2 gain and Hg bias are then used to strip the very small residual ^{204}Hg interference from ^{204}Pb (any variation in these parameters during the day is insignificant for the size of the correction being made). Then using the Pb mass bias determined as above and knowledge of the true $^{208}\text{Pb}/^{204}\text{Pb}$ ratio of NIST SRM 612 we can calculate a gain factor for IC0 by comparing the observed vs. expected ^{204}Pb signal. Ion counter gain measurements so determined are averaged throughout a given analytical session and this value is then used to correct all unknowns. In this way we can determine the gain on IC0 for any particular ablation to $\sim 0.2\%$ (total gain variation within any given day does not exceed $\pm 0.3\%$). Because of uncertainties associated with changing the ion beam steering during jumping routines, we believe that gains measured in this way are more accurate than those determined by either cycling an isotope pair into Faraday cups and ion counters, or cycling a single beam into each collector and referencing it back to the Faraday cup. The correction factors for mass bias and ion counter gain discussed above are determined on standard glass samples run intermittently during a given analytical session.

We now consider the measurement of samples. For those beams measured in an ion counter, the first data reduction step is a dead-time correction that is applied automatically for all analyses by the time-resolved analysis software supplied with the instrument, using the default dead-time. All subsequent data reduction is performed using the Wavemetrics waveform program Igor Pro and Microsoft Excel spreadsheets. In the initial stages of this work we encountered some errors related to the Tau correction applied to rapidly changing signals (the latter often encountered in laser ablation); these effects were similar in form to those documented by Hirata *et al.*,²² manifest as an apparent correlation between measured isotope ratio and rate of change of signal size. Although the Nu Plasma time-resolved software has now been modified to provide an improved Tau correction,²³ in order to utilise our early data and yet maintain consistency, we have applied the Tau correction manually for all samples and standards analysed in this study. After these two corrections to the raw data, the on-peak zeros are then subtracted from the on-peak integrations, and the ion counter signals are corrected with the externally determined gain. Importantly the on-peak zero correction removes almost all of the ^{204}Hg interference on ^{204}Pb . Any residual interference (either due to fluctuations in the background or to Hg derived from the sample itself, and which is now typically less than 1% of the signal at mass 204) is corrected using the ^{200}Hg monitor. ^{204}Hg is determined from ^{200}Hg , using the natural $^{204}\text{Hg}/^{200}\text{Hg}$ ratio of 0.2973²⁴ and a mass bias factor determined on the gas blank at the start of the day (minor variations in this factor have no influence on the correction at this level of interference). The ^{208}Pb , ^{207}Pb , and ^{206}Pb ion currents are then ratioed to ^{204}Pb or ^{206}Pb , where appropriate, and an outlier rejection ($> \pm 2$ s.d.; e.g. Mathez and Waight⁴) performed. The resultant means for each ratio are then bias corrected using an exponential law and the bias factor determined externally on NIST SRM 612.

Results and discussion

Precision and accuracy in theory and practice

Before discussing the observed results, it is pertinent to examine the theoretical limits of precision attainable to provide a benchmark against which to gauge the success of our results (see also Horstwood *et al.*⁸). The basic principles of such an

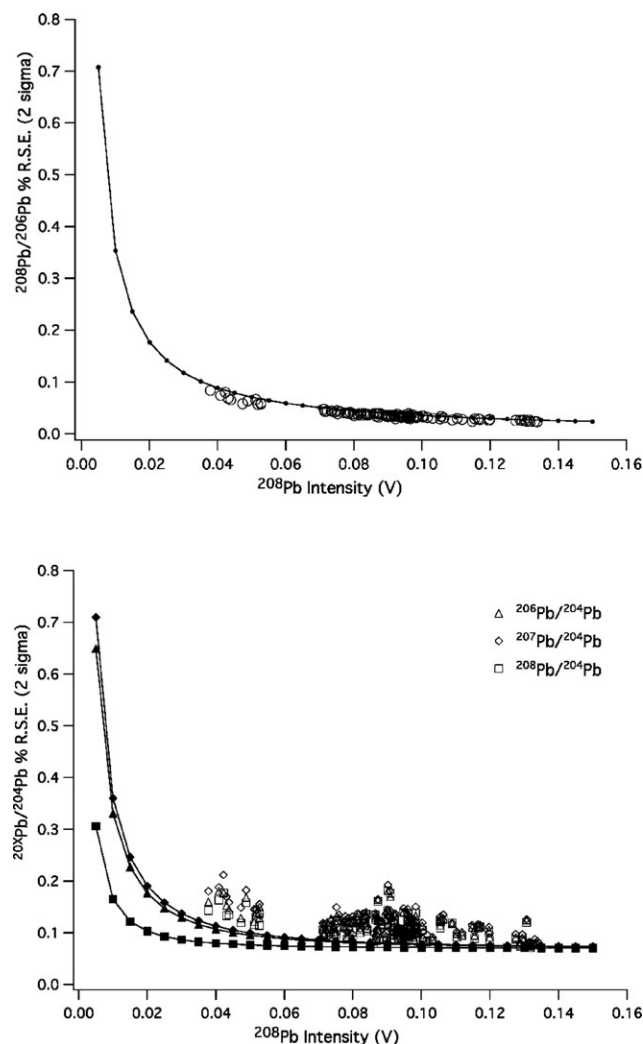


Fig. 2 Relative standard errors (RSEs) expressed as percentages relative to varying Pb beam intensities (using ^{208}Pb as a proxy for total Pb). Filled symbols represent theoretically determined values, unfilled symbols are observed RSEs for the NIST SRM 612 standard runs. Precision decreases exponentially at lower Pb levels. Collector noise for the ion counters used in theoretical calculations is $\sim 2 \times 10^{-8}$ V per 0.2 s.

analysis follow the work of Ludwig,²⁵ applied to the analytical protocol used in this paper, and adapted where necessary. In brief, the measurement of any perfectly stable beam will still have an inherent degree of uncertainty due to:

1. Counting statistics. In which $\sigma = \sqrt{n}$ where σ is the uncertainty at one standard deviation, and n is the total number of ions counted. See Fitzsimons *et al.*²⁶ for a comprehensive discussion of counting statistics.
2. Collector noise: all collectors have a degree of noise that will be superimposed on any signal measured. For Faraday cups, this noise will be the result of thermal noise on the high ohmic resistors,²⁵ governed by Johnson's Law.[†] Ion counters have inherent noise associated with dark current (see Platzner²⁴).
3. Zero measurement uncertainty. This is the uncertainty of a beam that has a zero measurement subtracted from it. The

[†] Johnson's Law states that $\sigma = \sqrt{\frac{4kT\Delta f}{R}}$ where σ is the collector noise (in amperes), k is the Boltzmann constant ($1.38 \times 10^{-23} \text{ J K}^{-1}$), T is the temperature (K), Δf is the measurement bandwidth ($= 5$ measurements per second in this study), and R is the resistance of the collector (10^{11} ohm). Under the conditions of this study, the collector noise, at 1 s.d. is approximately 90 microvolts per 0.2 s, using Ohm's law to convert amperes to volts.

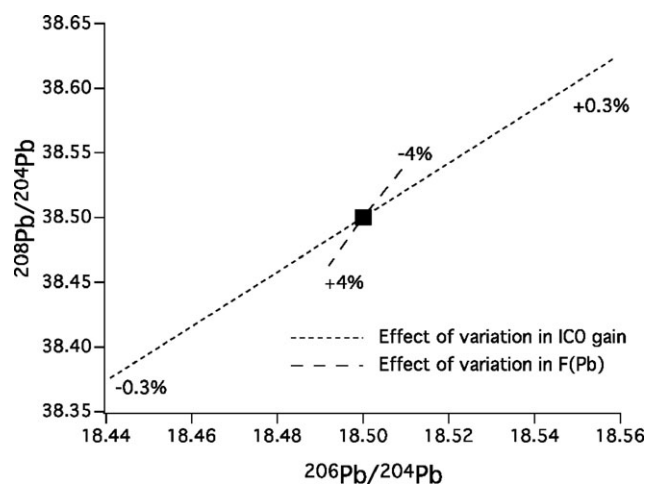


Fig. 3 The effects of variations in the lead fractionation correction and ion counter gain calibration, shown as percentage variation, on arbitrary $^{208}\text{Pb}/^{204}\text{Pb}$ and $^{206}\text{Pb}/^{204}\text{Pb}$ ratios of 38.5 and 18.5, respectively. It is clear that the ion counter gain plays the most important role in the accuracy of ratios involving ^{204}Pb .

zero measurement (or blank) is affected by both counting statistics and collector noise uncertainties.

Thus, for an isotope ratio, the resultant uncertainty can be given by:

$$s_{a/b} = (a/b) \times \sqrt{\left(\frac{s_a}{a}\right)^2 + \left(\frac{s_b}{b}\right)^2} \quad (1)$$

where $s_{a/b}$ is the uncertainty (at 1 s.d.) for the ratio of a/b , s_a and s_b are the blank corrected uncertainties for beams a and b , and a and b are the intensity of beams a and b , respectively (V). This represents the simplest case for two beams, both collected in Faraday cups *e.g.* $^{208}\text{Pb}/^{206}\text{Pb}$. A comparison of the theoretical precision calculated in this way for the experimental

Table 2 Solution and *in situ* values for the samples measured in this study^a

	$^{206}\text{Pb}/^{204}\text{Pb}$	$^{207}\text{Pb}/^{204}\text{Pb}$	$^{208}\text{Pb}/^{204}\text{Pb}$	$^{208}\text{Pb}/^{206}\text{Pb}$	$^{207}\text{Pb}/^{206}\text{Pb}$
BCR2-g $\sim 10 \mu\text{g g}^{-1} \text{ Pb}$ ($n = 70$)					
Sol value	18.770	15.622	38.722	2.063	0.832
Mean	18.757	15.619	38.750	2.066	0.833
$2 \times \text{s.d.}$	0.076	0.066	0.147	0.002	0.002
$2 \times \text{RSD}\%$	0.40	0.42	0.38	0.11	0.22
MPI-ATHO-G $\sim 6 \mu\text{g g}^{-1} \text{ Pb}$ ($n = 70$)					
Sol value	18.375	15.473	38.087	2.073	0.842
Mean	18.376	15.479	38.102	2.073	0.842
$2 \times \text{s.d.}$	0.111	0.091	0.183	0.006	0.004
$2 \times \text{RSD}\%$	0.60	0.59	0.48	0.30	0.47
MPI-KL2-G $\sim 2 \mu\text{g g}^{-1} \text{ Pb}$ ($n = 20$)					
Sol value	19.026	15.628	38.507	2.024	0.821
Mean	19.043	15.620	38.515	2.023	0.819
$2 \times \text{s.d.}$	0.272	0.276	0.566	0.014	0.009
$2 \times \text{RSD}\%$	1.43	1.76	1.47	0.70	1.06

^a All solution values are reported relative to the following values for NIST SRM 981, from Woodhead,¹⁰ which are within error of those obtained by Todt *et al.*:³² $^{206}\text{Pb}/^{204}\text{Pb} \sim 16.9356$, $^{207}\text{Pb}/^{204}\text{Pb} \sim 15.4891$, $^{208}\text{Pb}/^{204}\text{Pb} \sim 36.7006$. Comparison of these data with some other studies (*e.g.* Thirlwall,³³ Jochum *et al.*)²⁸ at high levels of precision may require re-normalisation to their preferred values for the SRM 981 Pb standard. Each sample was measured over two or more sessions during a period of several months, except MPI-KL2-G, which was measured only on one occasion.

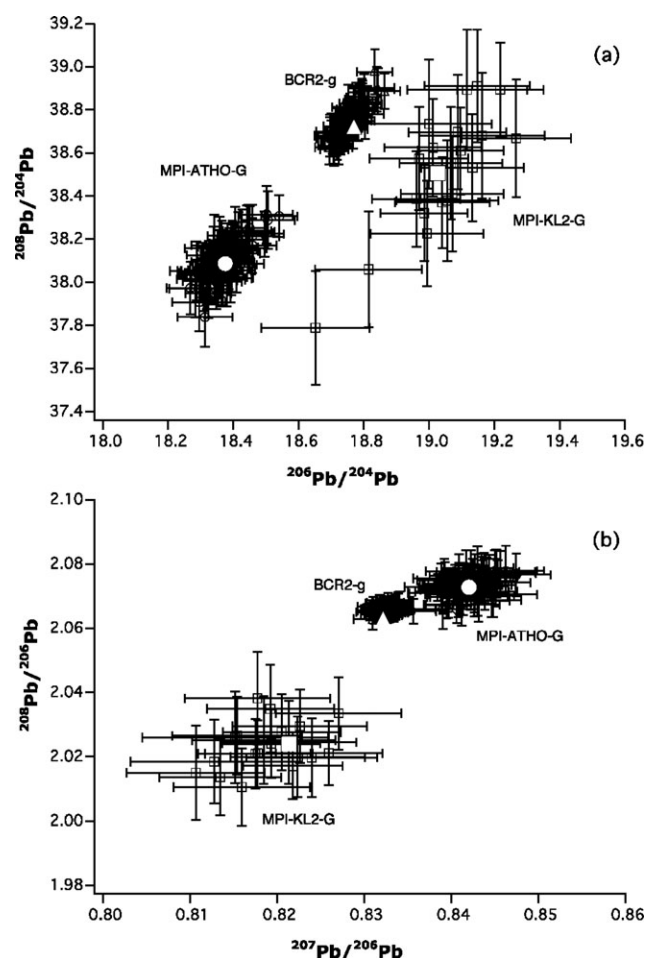


Fig. 4 The measured ratios of $^{208}\text{Pb}/^{204}\text{Pb}$ vs. $^{206}\text{Pb}/^{204}\text{Pb}$ (a), and $^{208}\text{Pb}/^{206}\text{Pb}$ vs. $^{207}\text{Pb}/^{206}\text{Pb}$ (b). Solution values, shown as larger white symbols, fall within the fields defined by the *in situ* analyses, except for BCR2-g which shows a systematic offset in its $^{208}\text{Pb}/^{206}\text{Pb}$ ratio, possibly due to isotopic heterogeneity in this standard.

conditions with the observed internal analytical precision is provided in Fig. 2(a). The observed internal precision appears to be slightly lower than the theoretical, due to the outlier rejection procedure. This effect is negligible, and overall the observed precision correlates well with the theoretical. The exponential nature of the curve in Fig. 2(a) suggests that data quality will rapidly degrade if ^{208}Pb signals fall below 0.03 V and, if maintained above this level, the ultimate precision attainable on $^{208}\text{Pb}/^{206}\text{Pb}$ for realistic beam sizes would be $\sim 0.05\%$ (2 sigma).

Due to the mercury interference on $m/z = 204$, and the ion counter gain calibration, calculation of the theoretical limits of precision for ratios involving ^{204}Pb is more complex. Firstly, the blank corrected uncertainties for ^{204}X and ^{200}Hg are calculated in an analogous manner to $^{208}\text{Pb}/^{206}\text{Pb}$ and $^{207}\text{Pb}/^{206}\text{Pb}$. The uncertainty in the amount of ^{204}Hg ($s_{\text{Hg}204}$) will also depend on the mercury fractionation factor, determined each session using the cell-gas blank.

Ultimately, the ^{204}Pb signal uncertainty is given by:

$$s_{204\text{Pb}}^2 = s_{\text{GB}204}^2 + s_{\text{Hg}204}^2 \quad (2)$$

where $s_{204\text{Pb}}$ is the uncertainty for ^{204}Pb and $s_{\text{GB}204}$ is the gain and blank corrected uncertainty for ^{204}X .

The analytical uncertainty, at 1σ , for a ^{204}Pb denominated ratio, is then determined using eqn (1) where $b = ^{204}\text{Pb}$, calculated from ^{204}X , and $s_b = s_{204\text{Pb}}$. For this case, the observed compared to predicted analytical uncertainty is shown in Fig. 2(b). The observed precision is now slightly larger than the theoretical.

The two primary controls on analytical accuracy using this method are the quality of our measurements of instrumental mass bias and ion counter gain which, as noted above, are determined externally by reference to analyses of NIST 612 glass. Fig. 3 shows how inaccuracies in the measurement of these two factors propagate into the final isotope results. As we have noted previously our estimate of the instrumental mass bias is unlikely to be in error by more than ± 0.05 on a typical '*F*' value of -1.25 ($\sim 4\%$), for example. Such errors would result in relatively minor changes in the calculated $^{206}\text{Pb}/^{204}\text{Pb}$ ratio of $\pm 0.05\%$. In contrast we conservatively suggest that we can externally determine the IC0 gain confidently to only $\pm 0.3\%$ and variations of this size result in quite marked changes to the calculated $^{206}\text{Pb}/^{204}\text{Pb}$ ratio of $\pm 0.32\%$. This is a clear demonstration that the ultimate accuracy of Pb-isotope determinations involving the ^{204}Pb isotope is very strongly influenced by the estimation of ion counter gain. Using any of the methods noted above it is difficult to determine such gains to better than 0.1% and this therefore represents a fundamental limit on the accuracy of *in situ* Pb-isotope determinations by mixed Faraday-ion counter methods. Much of this uncertainty could be reduced by cycling all isotopes of interest through a single ion counter but the time penalty incurred by such an approach would be unacceptable for our purposes (melt inclusion analysis) where all the sample may be exhausted in less than 1 minute of ablation. Any errors

arising in the mercury correction, either from variations in the $^{204}\text{Hg}/^{200}\text{Hg}$ ratio or the mercury fractionation factor, are of the order of 0.01% , and are much too small to be shown in Fig. 3. Such inaccuracies will affect the observed ratios in the same ways as uncertainties in IC0 gain, and the two cannot be deconvolved.

Three reference glasses of variable Pb content were employed in this study to test the efficacy of our analytical protocol: BCR2-g (*e.g.* Rocholl²⁷), ATHO-G and KL2-G (MPI-DING).²⁸ The chemistry of the basalt glass standard BCR2-g has been documented by Eggins²⁰ and contains approximately $10 \mu\text{g g}^{-1}$ Pb. ATHO-G is a glass of rhyolitic composition and has a Pb concentration of $5.5 \mu\text{g g}^{-1}$.²⁹ The lowest Pb concentration sample used ($\sim 2.2 \mu\text{g g}^{-1}$) was a basaltic glass, KL2-G. These three glasses, which we analysed as 'unknowns' thus cover a range of Pb concentrations and matrix compositions. The lead isotopic compositions of these samples, as measured by conventional solution methods in our laboratory, are presented in Table 2, together with the isotopic ratios measured by laser ablation analysis.

A comparison of the solution-based analyses with those obtained by laser ablation (Fig. 4) demonstrates that for all samples, the laser ablation data are within error of the solution values, except for the $^{208}\text{Pb}/^{206}\text{Pb}$ ratio of BCR2-g. This ratio is consistently higher when measured by laser ablation, despite its high relative precision and raises the possibility of isotopic

Table 3 Comparison of accuracies for various instruments and standards^a

	Authors	System	Sample	Amount of sample consumed	Pb conc./ $\mu\text{g g}^{-1}$	Ratio	Accuracy (%)
Radiogenic lead	Horn <i>et al.</i> ⁵	ICP-QMS	91500 Zircon	0.1–10 μg	~ 14	$^{208}\text{Pb}/^{206}\text{Pb}$	4.92
			SL13 Zircon	0.1–10 μg	N/A	$^{207}\text{Pb}/^{206}\text{Pb}$	3.11
	Horstwood <i>et al.</i> ⁸	MC-ICP-MS	Various monazite standards	$5.4 \times 10^{-4} \text{ cm}^3$	N/A	$^{207}\text{Pb}/^{206}\text{Pb}$	3.93
Common lead	Aries <i>et al.</i> ³⁰	ICP-QMS	Lake sediment cores	$> 7.5 \times 10^{-4} \text{ cm}^3$	> 20	$^{206}\text{Pb}/^{204}\text{Pb}$	0.35
						$^{207}\text{Pb}/^{204}\text{Pb}$	0.33
						$^{208}\text{Pb}/^{206}\text{Pb}$	0.14
	Crowe <i>et al.</i> ³¹	ICP-QMS	NIST 614	$1.8 \times 10^{-3} \text{ cm}^3$	~ 2	$^{207}\text{Pb}/^{206}\text{Pb}$	0.7
	Jochum <i>et al.</i> ²⁸	ICP-QMS	MPI-DING Standard glasses		≥ 1	$^{208}\text{Pb}/^{206}\text{Pb}$	0.2–2
	Willigers <i>et al.</i> ¹⁹	MC-ICP-MS	NIST 610	$7.5 \times 10^{-7} \text{ cm}^3$	426	$^{206}\text{Pb}/^{204}\text{Pb}$	0.04
This study						$^{207}\text{Pb}/^{204}\text{Pb}$	0.05
						$^{208}\text{Pb}/^{206}\text{Pb}$	0.10
		MC-ICP-MS	BCR2-g ($n = 70$)	$4.3 \times 10^{-7} \text{ cm}^3$ ($\sim 1 \mu\text{g}$)	~ 10	$^{206}\text{Pb}/^{204}\text{Pb}$	0.21
						$^{207}\text{Pb}/^{204}\text{Pb}$	0.21
						$^{208}\text{Pb}/^{204}\text{Pb}$	0.20
						$^{208}\text{Pb}/^{206}\text{Pb}$	0.16
						$^{207}\text{Pb}/^{206}\text{Pb}$	0.12
			MPI-ATHO-G	$4.3 \times 10^{-7} \text{ cm}^3$ ($\sim 1 \mu\text{g}$)	~ 6	$^{206}\text{Pb}/^{204}\text{Pb}$	0.30
						$^{207}\text{Pb}/^{204}\text{Pb}$	0.30
						$^{208}\text{Pb}/^{204}\text{Pb}$	0.24
						$^{208}\text{Pb}/^{206}\text{Pb}$	0.15
						$^{207}\text{Pb}/^{206}\text{Pb}$	0.24
			MPI-KL2-G	$4.3 \times 10^{-7} \text{ cm}^3$ ($\sim 1 \mu\text{g}$)	~ 2	$^{206}\text{Pb}/^{204}\text{Pb}$	0.72
						$^{207}\text{Pb}/^{204}\text{Pb}$	0.88
						$^{208}\text{Pb}/^{204}\text{Pb}$	0.74
						$^{208}\text{Pb}/^{206}\text{Pb}$	0.35
						$^{207}\text{Pb}/^{206}\text{Pb}$	0.61

^a Note: studies of radiogenic lead may involve ratios radically different from those measured in common lead studies.

heterogeneity in this sample, a suggestion which can only be tested by further *in situ* measurements. Since mass bias was corrected by an external normalisation, our data reveal that at least for the analysis of glasses, any matrix effects related to the composition of the glass are insignificant at these levels of analytical precision. The external precision, or reproducibility, is correlated with Pb content and, for ratios involving ^{204}Pb , varies from 0.4% RSD (2 sigma) at 10 ppm to ~2% RSD (2 sigma) at 2 ppm.

Amount of sample consumed/system efficiency

The drill-rate for a variety of laser output energies, at constant spot size, was determined for a NIST glass sample using a calibrated microscope fitted with sub-micron stepper-motor stage movement. The results for these conditions are shown in Fig. 5, and are not expected to change substantially for most sample glasses. At typical operating conditions for this study (~46 mJ output energy), the drill rate is thus approximately $0.18\ \mu\text{m pulse}^{-1}$. A pit of ~63 μm depth should result from a 6 Hz repetition rate, for 60 seconds ablation time. The volume of material ablated would therefore be in the order of $4.3 \times 10^{-7}\ \text{cm}^3$, which, if the density of the material is assumed to be approximately $2.4\ \text{g cm}^{-3}$ (Walder *et al.*¹ value for NIST SRM 610), is approximately one microgram of sample consumed. This equates to a sampling efficiency (*i.e.* ions counted/atoms ablated) of 0.6%, almost three times that noted by Walder *et al.*¹ on NIST glass using a Nd-YAG laser operating at 266 nm.

Comparison with previous studies

Comparisons between techniques are difficult to make, due to the use of varying instruments, analytical conditions, standards and protocols. Table 3, however, presents a summary of results obtained by other authors, which can be contrasted with the results of this study.

Compared to quadrupole mass spectrometry (LA-ICP-QMS)^{5,30,31} where sensitivity is generally lower and thus larger (up to $3 \times 10^{-3}\ \text{cm}^3$) amounts of sample are required to obtain accuracies of >0.3% for $^{206}\text{Pb}/^{204}\text{Pb}$ and $^{207}\text{Pb}/^{204}\text{Pb}$, this study provides a dramatic improvement. The use of multi-collection instrumentation drastically improves both the precision and accuracy of isotope ratio measurements, however. For example, Mathez and Waight⁴ quote the mean of their laser ablation measurements of NIST SRM 610 as being within 0.06%, 0.09%, 0.19%, 0.12% and 0.02% of the TIMS value for the ratios $^{206}\text{Pb}/^{204}\text{Pb}$, $^{207}\text{Pb}/^{204}\text{Pb}$, $^{208}\text{Pb}/^{204}\text{Pb}$, $^{208}\text{Pb}/$

^{206}Pb and $^{207}\text{Pb}/^{206}\text{Pb}$, respectively. These data are comparable to those obtained in this study but required the use of longer integration times (100 s vs. 60 s), larger beam diameters (200 μm vs. 93 μm) and higher pulse rates (20 Hz vs. 6 Hz), and were obtained on materials with approximately 40 times higher lead concentration ($426\ \mu\text{g g}^{-1}\ \text{Pb}$ (NIST 610)⁴ *cf.* $\sim 10\ \mu\text{g g}^{-1}\ \text{Pb}$ (BCR2-g)). Considering all these factors we would suggest that the technique described herein provides a significant improvement over all previous studies.

Conclusions

A new method is described for the analysis of low Pb (1–10 $\mu\text{g g}^{-1}$) materials by laser ablation MC-ICP-MS. The use of parallel ion counters to measure Hg-corrected ^{204}Pb allows the determination of five Pb isotopic ratios, compared to the two ratios quoted in most previous studies. External mass bias correction and ion counter gain calibration, using NIST SRM 612, provides Pb isotopic ratios comparable to solution values, and which approach theoretical limits of precision. The measurement of ^{204}Pb in low-Pb samples opens the use of LA-ICP-MS to a greater range of applications, whilst improvements in the accuracy of $^{207}\text{Pb}/^{206}\text{Pb}$ determinations will lead to more accurate dating of minerals *in situ*.

Acknowledgements

We would like to thank J. Hellstrom and K. Ludwig for their insightful discussion and helpful suggestions. R. Kemp's help in programming IgorTM is also greatly appreciated.

References

- 1 A. J. Walder, I. D. Abell, I. T. Platzner and P. A. Freedman, *Spectrochim. Acta, Part B*, 1993, **48B**, 397–402.
- 2 B. J. Fryer, S. E. Jackson and H. P. Longerich, *Chem. Geol.*, 1993, **109**, 1–8.
- 3 M. Ponting, J. A. Evans and V. Pashley, *Archaeometry*, 2003, **45**, 591–597.
- 4 E. A. Mathez and T. E. Waight, *Geochim. Cosmochim. Acta*, 2003, **67**, 1875–1888.
- 5 I. Horn, R. L. Rudnick and W. F. McDonough, *Chem. Geol.*, 2000, **164**, 281–301.
- 6 T. Andersen, *Chem. Geol.*, 2002, **192**, 59–79.
- 7 S. E. Jackson, N. J. Pearson, W. L. Griffin and E. A. Belousova, *Chem. Geol.*, 2004, **211**, 47–69.
- 8 M. S. A. Horstwood, G. L. Foster, R. R. Parrish, S. R. Noble and G. M. Nowell, *J. Anal. At. Spectrom.*, 2003, **18**, 837–846.
- 9 S. M. Eggins, L. P. J. Kinsley and J. M. G. Shelley, *Appl. Surf. Sci.*, 1998, **127–129**, 278–286.
- 10 J. D. Woodhead, *J. Anal. At. Spectrom.*, 2002, **17**, 1–6.
- 11 J. D. Woodhead, J. M. Hergt, M. Shelley, S. M. Eggins and R. Kemp, *Chem. Geol.*, 2004, **209**, 121–135.
- 12 J. D. Woodhead, S. Swearer, J. M. Hergt and R. Maas, *J. Anal. At. Spectrom.*, 2005, **20**, 22–27.
- 13 D. Günther and C. A. Heinrich, *J. Anal. At. Spectrom.*, 1999, **9**, 1363–1368.
- 14 J. D. Woodhead, F. Volker and M. T. McCulloch, *Analyst*, 1995, **120**, 35–39.
- 15 M. F. Thirlwall, *Chem. Geol.*, 2000, **163**, 299–322.
- 16 J. Baker, D. Peate, T. Waight and C. Meyzen, *Chem. Geol.*, 2004, **211**, 275–303.
- 17 H. P. Longerich, B. J. Fryer and D. F. Strong, *Spectrochim. Acta, Part B*, 1987, **42**, 39–48.
- 18 M. Tiepolo, *Chem. Geol.*, 2003, **199**, 159–177.
- 19 B. J. A. Willigers, J. A. Baker, E. J. Krogstad and D. W. Peate, *Geochim. Cosmochim. Acta*, 2002, **66**, 1051–1066.
- 20 S. M. Eggins, *Geostand. Newsl.*, 2003, **27**, 147–162.
- 21 J. D. Woodhead and J. M. Hergt, *Geostand. Newsl.*, 2001, **25**, 261–266.
- 22 T. Hirata, Y. Hayano and T. Ohno, *J. Anal. At. Spectrom.*, 2003, **18**, 1283–1288.
- 23 P. A. Freedman, personal communication, 2005.
- 24 I. T. Platzner, *Modern Isotope Ratio Mass Spectrometry*, John Wiley & Sons Inc., West Sussex, 1997, 514.
- 25 K. R. Ludwig, *US Geol. Surv. Bull.*, 1986, **B1622T**, 219–221.

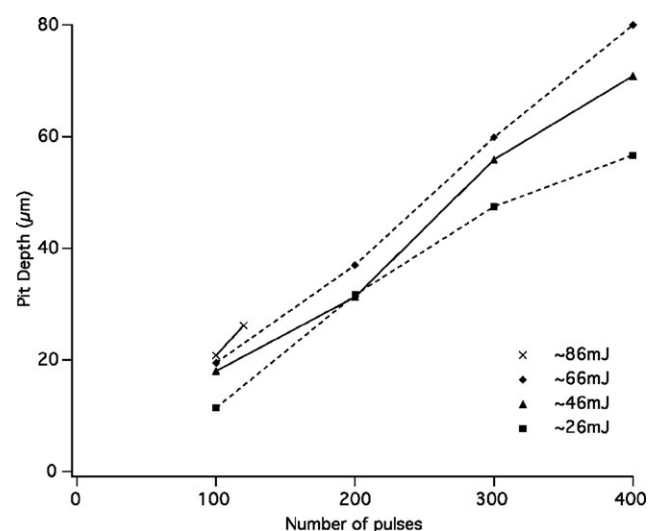


Fig. 5 Pit depths for varying laser energies using a spot size of 93 μm . The ~46 mJ setting was used during the reported analytical sessions, and equates to a drill rate of approximately $0.18\ \mu\text{m pulse}^{-1}$.

- 26 I. C. W. Fitzsimons, B. Harte and R. M. Clark, *Mineral. Mag.*, 2000, **64**, 59–83.
- 27 A. Rocholl, *Geostand. Newsl.*, 1998, **22**, 33–45.
- 28 K. P. Jochum, B. Stoll, K. Herwig, B. Amini, W. Abouchami and A. W. Hofmann, *Int. J. Mass Spectrom.*, 2005, **242**, 281–289.
- 29 L. Halicz and D. Günther, *J. Anal. At. Spectrom.*, 2004, **19**, 1539–1545.
- 30 S. Aries, M. Motelica-Heino, R. Freydier, T. Grezes and M. Polvé, *Geostand. Newsl.*, 2001, **25**, 387–398.
- 31 S. A. Crowe, B. J. Fryer, I. M. Samson and J. E. Gagnon, *J. Anal. At. Spectrom.*, 2003, **18**, 1331–1338.
- 32 W. Todt, R. A. Cliff, A. Hanser and A. W. Hofmann, in *Earth Processes: Reading the Isotopic Code*, ed. A. R. Basu and S. R. Hart, American Geophysical Union Monograph, 1996, **95**, 429–437.
- 33 M. F. Thirlwall, *Chem. Geol.*, 2002, **184**, 255–279.